Author's personal copy

Ecological Indicators 26 (2013) 117–125

Contents lists available at SciVerse ScienceDirect

Ecological Indicators

journal homepage: www.elsevier.com/locate/ecolind

Estimating the spatial pattern of soil respiration in Tibetan alpine grasslands using Landsat TM images and MODIS data

Ni Huang[a,*], Jin-Sheng He[b,c], Zheng Niu[d]

[a] The State Key Laboratory of Remote Sensing Science, Institute of Remote Sensing and Digital Earth, Chinese Academy of Sciences, Beijing 100101, China
[b] Department of Ecology and Key Laboratory for Earth Surface Processes of the Ministry of Education, Peking University, 5 Yiheyuan Rd., 100871 Beijing, China
[c] Key Laboratory of Adaptation and Evolution of Plateau Biota, Northwest Institute of Plateau Biology, Chinese Academy of Sciences, 23 Xinning Rd., Xining 810008, China
[d] The State Key Laboratory of Remote Sensing Science, Laboratory of Digital Earth Sciences, Institute of Remote Sensing and Digital Earth, Chinese Academy of Sciences, Beijing 100094, China

ARTICLE INFO

Article history:
Received 9 April 2012
Received in revised form 19 October 2012
Accepted 28 October 2012

Keywords:
Remote sensing
Biomass
Vegetation indices
Soil respiration
Alpine grasslands
Landsat TM
MODIS

ABSTRACT

Monitoring soil respiration (R_s) at regional scales using images from operational satellites remains a challenge because of the problem in scaling local R_s to the regional scales. In this study, we estimated the spatial distribution of R_s in the Tibetan alpine grasslands as a product of vegetation index (VI). Three kinds of vegetation indices (VIs), that is, normalized difference vegetation index (NDVI), enhanced vegetation index (EVI), and modified soil adjusted vegetation index (MSAVI), derived from Landsat Thematic Mapper (TM) and Moderate-resolution Imaging Spectroradiometer (MODIS) surface reflectance product were selected to test our method. Different statistical models were used to analyze the relationships among the three VIs and R_s. The results showed that, based on the remote sensing data from either MODIS or Landsat TM, exponential function was the optimal fit function for describing the relationships among VIs and R_s during the peak growing season of alpine grasslands. Additionally, NDVI consistently showed higher explanation capacity for the spatial variation in R_s than EVI and MSAVI. Thus, we used the exponential function of TM-based NDVI as the R_s predictor model. Since it is difficult to achieve full spatial coverage of the entire study area with Landsat TM images only, we used the MODIS 8-day composite images to obtain the spatial extrapolation of plot-level R_s after converting the NDVI_MODIS into its corresponding NDVI_TM. The performance of the R_s predictor model was validated by comparing it with the field measured R_s using an independent dataset. The TM-calibrated MODIS-estimated R_s was within an accuracy of field measured R_s with R^2 of 0.78 and root mean square error of 1.45 gC m^{-2} d^{-1}. At the peak growing season of alpine grasslands, R_s was generally much higher in the southeastern part of the Tibetan Plateau and gradually decreased toward the northwestern part. Satellite remote sensing demonstrated the potential for the large scale mapping of R_s in this study.

© 2012 Elsevier Ltd. All rights reserved.

1. Introduction

Soil respiration (R_s) is an important process in the carbon cycle of terrestrial ecosystems (Raich and Schlesinger, 1992). At an annual scale, R_s is estimated to contribute around 75×10^{15} gC $year^{-1}$ to the global carbon budget and is second only to oceans in the magnitude of the gross CO_2 flux to the atmosphere (Schlesinger and Andrews, 2000). Thus, small changes in the rate of R_s may alter the annual C sink of terrestrial ecosystems (Cox et al., 2000; Trumbore, 2006). Accurately estimating R_s, as well as determining the effect of ecological factors on R_s, is the key to evaluating the role of soil biological processes in ecosystem carbon cycling (Fang et al., 1998; Craine et al., 1999; Chen et al., 2011).

R_s is not entirely produced by the decomposition of soil organic matter (SOM) (Kuzyakov and Larionova, 2005). As most soils are covered with vegetation, root-derived CO_2 contributes to CO_2 efflux from the soil as well. Photosynthesis stimulates R_s after the translocation of the recent photosynthate to roots and root-associated soil microbes (Moyano et al., 2007). Although large amounts of fresh carbon supply from photosynthesis serve as substrate for respiration, they may inhibit the decomposition of plant residues (de Graaff et al., 2010) and determine the SOM decomposition (Balogh et al., 2011). Bader and Cheng (2007) also found that the temperature response of R_s is mediated by fresh carbon supply or by current photosynthesis capacity. Therefore, R_s is closely correlated with current photosynthesis, which has been demonstrated clearly by previous studies (Högberg et al., 2001; Pendall et al., 2001; Tang et al., 2005; Moyano et al., 2007). Because large surveys of plant photosynthesis are virtually impossible to conduct at the regional scale, a proxy for plant photosynthesis, which can

* Corresponding author. Tel.: +86 10 648 895 61; fax: +86 10 648 062 58.
E-mail address: huangni84@gmail.com (N. Huang).

1470-160X/$ – see front matter © 2012 Elsevier Ltd. All rights reserved.
http://dx.doi.org/10.1016/j.ecolind.2012.10.027

Author's personal copy

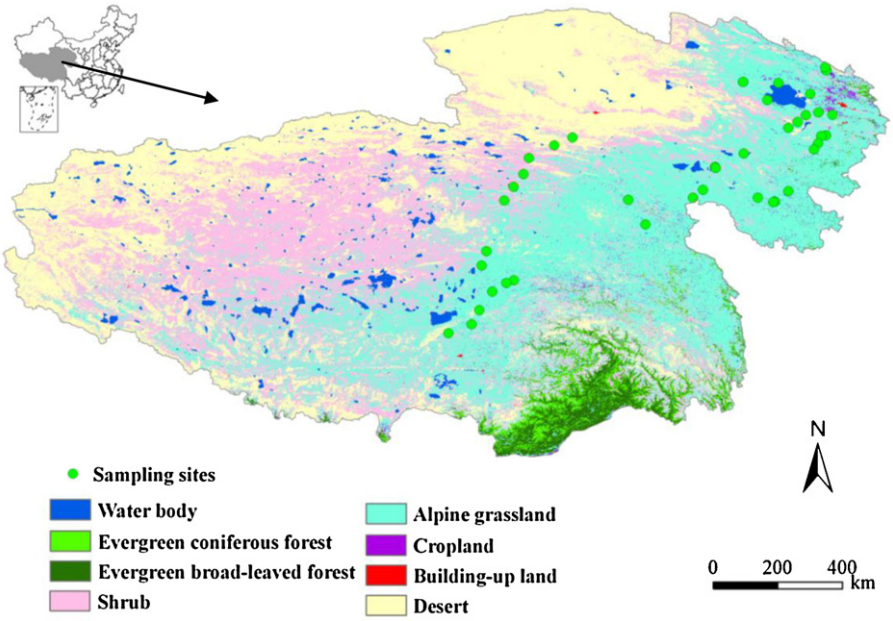

Fig. 1. Field sampling sites of soil respiration during the peak growing season of alpine grasslands, and land cover data from MODIS in the Tibetan Plateau in 2006.

explain the spatial variations in R_S, is required. The plant biomass is a good candidate, because it can strongly influence the rate of R_S (Fang et al., 1998; Han et al., 2007; Geng et al., 2012).

An understanding of grassland C dynamics is essential to clarify the contribution of grassland ecosystems to the global C budget (Scurlock and Hall, 1998). When greenness is near peak value in annual grassland communities, biomass and photosynthesis both reach the maximum and are closely related (Reeves et al., 2006). At the peak growing season of alpine grasslands in the Tibetan Plateau, belowground biomass is found to be the most important driving factor for large-scale variations in R_S (Geng et al., 2012).

Through measuring the reflected radiation from plant canopies, remote sensing techniques can be used to evaluate the biophysical parameters of plants within the sensor's field of view (Guo et al., 2011). The application of remote sensing in grasslands worldwide has been especially successful because of the relative structural simplicity of these ecosystems (versus, for example, that of woodlands or forests), as well as the tendency of the grasslands, especially those dominated by annual grasses, to be green for a significant fraction of the year (Wylie et al., 2002; Butterfield and Malmstrom, 2009). Numerous studies have shown that vegetation indices such as the normalized difference vegetation index (NDVI) can be strongly correlated with grassland biomass (Brinkmann et al., 2011) and are often used as tools for detecting and quantifying large-scale changes in grassland processes associated with global change (Cleland et al., 2006; Brinkmann et al., 2011; Ouyang et al., 2012). To date, limited studies have incorporated satellite-level remote-sensing data and R_S measured in the field. Thus, examining whether satellite-level remote-sensing data can be used to estimate R_S is necessary.

Landsat data with high spatial resolution have proven extremely useful in monitoring changes in land surfaces (Vogelman et al., 2001), but the 16-day revisit cycle and frequent cloud contamination have limited the application of Landsat over a large spatial scale, especially in regions with very unstable atmospheric conditions (e.g. Tibetan Plateau). The Terra or Aqua Moderate-resolution Imaging Spectroradiometer (MODIS) provides frequent coarse-resolution observations and is crucial for the timely monitoring of larger region. Thus, combining the Landsat and the MODIS data may be useful in monitoring the spatial distribution of R_S across a large area. This research explores the feasibility of using the multispectral Landsat TM images and MODIS data in predicting spatial patterns of R_S in the mid-growing season of alpine grasslands in the Tibetan Plateau. The primary objective of this study is to determine the application of broadband VIs, which can be estimators of plant biomass, to explain the spatial variation in R_S of the alpine grasslands in the Tibetan Plateau.

2. Methods

2.1. Study area

This study area is located in Qinghai-Xizang (Tibetan) Plateau in Southwest China (78.3°–103.1°E, 26.5°–39.5°N). The Tibetan Plateau is the highest and largest plateau on earth, with a mean elevation of about 4 km above sea level (asl). The mean annual temperature on the plateau is only 1.6 °C and its annual precipitation is around 413 mm (Yang et al., 2009). Greater than 60% of the plateau is covered by natural alpine grasslands (alpine steppe and meadow) (Li and Zhou, 1998). Moreover, a large part of the plateau has not been disturbed by human activities. Within the distribution area of alpine grasslands, 42 sites were selected for R_S measurements along a transect which stretches from 30.31 to 37.69°N and 90.80–101.48°E, and elevations from 2.925 to 5.105 km asl during late July and mid-August of 2006 (Fig. 1), when high convective activity and monsoon precipitation were concentrated (Yang et al., 2007). A detailed description of the sample sites can be found in Geng et al. (2012).

2.2. Field measurements

At each field measurement site, the sample data included diurnal soil respiration rate (R_S), soil temperature at 0–10 cm depth (T_S), soil moisture at 0–5 cm depth (SM), aboveground biomass (AGB) and belowground biomass (BGB). The detailed description of the field sampling design and the field data collection protocol can be found in Geng et al. (2012).

2.3. Remote sensing data

The Landsat Level 1 terrain corrected images (L1T, resolution = 30 m) were recorded by Landsat-5 TM instrument, and were

Author's personal copy

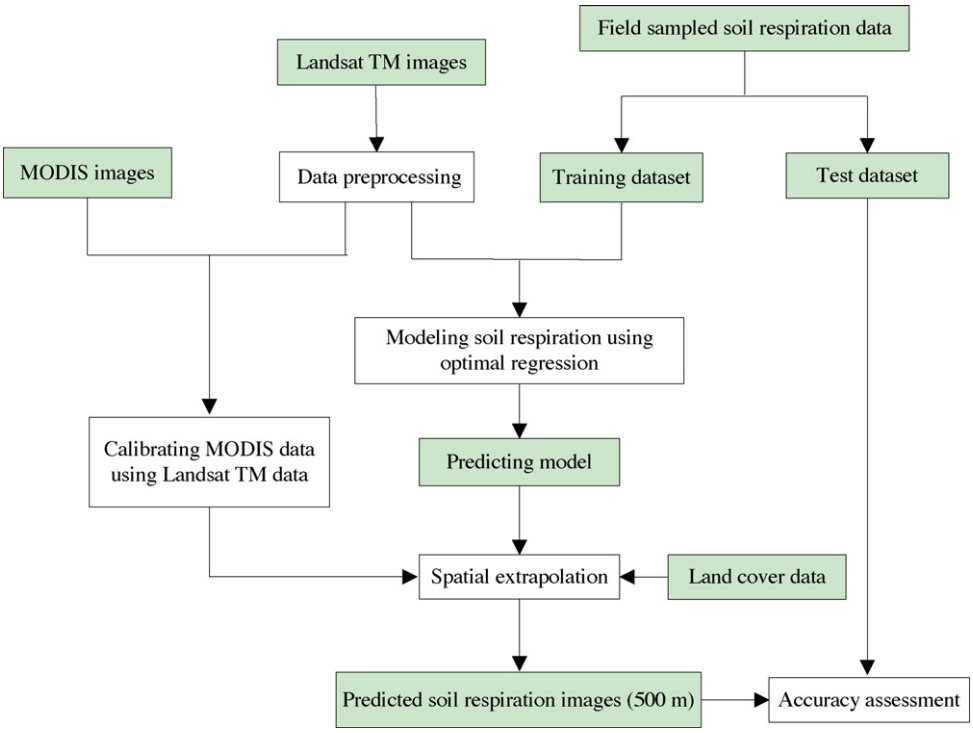

Fig. 2. A flow chart for deriving 500 m soil respiration during the peak growing season of alpine grasslands on the Tibetan Plateau in 2006. Data layers and models are in the green boxes and operation procedures in the white boxes. (For interpretation of the references to color in this figure caption, the reader is referred to the web version of the article.)

obtained from the US Geological Survey's Earth Resources Observation and Science. We used the TM images which were temporally close to the measurement time of the field samples to minimize the effects of changing ground conditions. Only cloud-free images of the sampling sites were used and all images were converted into reflectance. The pre-processing of TM images such as radiometric calibration, atmospheric correction, and geometric correction was accomplished using the Environment for Visualizing Images (ENVI) software. The detailed description of imagery procession can be found in Huang et al. (2010).

MODIS 8-day surface reflectance product (MOD09A1, 500 m) was downloaded (http://ladsweb.nascom.nasa.gov/data/search.html) for the Tibetan Plateau during the peak growing season (late July to mid-August) of 2006. Each MOD09A1 pixel contains the best possible observation during an 8-day period as selected on the basis of high observation coverage, low view angle, the absence of clouds or cloud shadow, and aerosol loading.

2.4. Vegetation indices calculation

VIs derived from satellite sensors (i.e. Landsat and MODIS) were used to estimate biomass and R_s of alpine grasslands in the Tibetan Plateau. The most known and widely used vegetation index (VI) is the NDVI developed by Rouse et al. (1974). Using satellite-derived reflectance data, this index was quantified by the following equation:

$$\mathrm{NDVI} = \frac{R_{\mathrm{Nir}} - R_{\mathrm{Red}}}{R_{\mathrm{Nir}} + R_{\mathrm{Red}}} \quad (1)$$

where R_x is the reflectance at the given wavelength (nm).

Despite its intensive use, the relationship between the NDVI and the vegetation biophysical parameters is known to be strongly affected by soil reflectance in sparsely vegetated areas and saturates in cases of dense and multi-layered canopy (Huete et al., 2002). Therefore, improved indices like the enhanced vegetation index (EVI; Huete et al., 2002) and the modified soil adjusted vegetation index (MSAVI; Qi et al., 1994) were calculated for comparison. The EVI (Eq. (2)) was proposed to use the blue band to primarily account for atmospheric correction, variable soil, and canopy background reflectance.

$$\mathrm{EVI} = 2.5 \times \frac{R_{\mathrm{Nir}} - R_{\mathrm{Red}}}{1 + R_{\mathrm{Nir}} + 6 \times R_{\mathrm{Red}} - 7.5 \times R_{\mathrm{Blue}}} \quad (2)$$

MSAVI (Eq. (3)) was suggested as an improvement over soil adjusted vegetation index (SAVI; Huete, 1988). This index is based on the concept of soil line, which describes the typical signatures of soils in a red or infrared bi-spectral plot and is obtained through the linear regression of the near-infrared band against the red band for a sample of bare soil pixels.

$$\mathrm{MSAVI} = \frac{2R_{\mathrm{Nir}} + 1 - \sqrt{(2R_{\mathrm{Nir}} + 1)^2 - 8(R_{\mathrm{Nir}} - R_{\mathrm{Red}})}}{2} \quad (3)$$

2.5. Land cover data

The land cover map of the Tibetan Plateau in 2006 was obtained from the Terra + Aqua MODIS Land Cover Type product (MCD12Q1, 500 m, http://ladsweb.nascom.nasa.gov/data/search.html) (Fig. 1). MCD12Q1 includes 11 natural vegetation classes, three developed and mosaicked land classes, and three non-vegetated land classes. Based on this land cover data, we extracted the types of grasslands in the Tibetan Plateau for our data analysis.

2.6. Regional extrapolation of soil respiration

In this study, we present a scaling-up technique to obtain information on R_s of alpine grasslands in the Tibetan Plateau. The overall approach consists of three key steps: analyzing the relationships among the VIs (NDVI, EVI and MSAVI) and the R_s from field measurements and determining the optimum R_s prediction model,

Author's personal copy

calibrating MODIS VI using Landsat TM VI, and then extrapolating the developed model spatially using 500 m resolution MODIS images (Fig. 2). The detailed procedure of data processing is given as follows:

Step 1: We separated the observed data into two datasets by using a random generator. One dataset had 30 samples for building a model, and the other had 12 samples for testing the model. We focused on analyzing the relationships between R_S and VIs based on the MODIS and TM images using linear, logarithmic, power, and exponential functions. Then we selected the optimal fit function which had the highest coefficient of determination as the R_S prediction model.
Step 2: Landsat TM images are difficult to achieve the full coverage of the study area, mainly suffered from the effect of long revisit cycle and cloud contamination. Thus, we converted the MODIS VI to the TM VI. Then we used the R_S prediction model to estimate R_S from 8-days composition MODIS images at each pixel to produce the spatial distribution of R_S for the whole study area.
Step 3: By overlapping the spatial distribution of alpine grasslands from the land cover data with R_S distribution map from the MODIS, we derived the spatial distribution of R_S for alpine grasslands in the Tibetan Plateau. Then, we evaluated the accuracy of prediction of simulated R_S using the independent test dataset.

2.7. Statistical analyses

Prior to statistical analyses, the parameters were tested for normality. Pearson correlation coefficient (r) was calculated to describe the relationships among R_S and related biotic and abiotic factors (i.e. AGB, BGB, SM, and T_S). Linear and nonlinear regression analyses were used to examine the relationships among the VIs (NDVI, EVI, and MSAVI), R_S, AGB, and BGB. The coefficient of determination (r^2) was used to evaluate the performance of the R_S models. The higher the r^2 values the better will be the fit to the observed data. All our statistical analyses were carried out using the SPSS 13.0 software package (SPSS, Chicago, IL, USA).

Table 1
Pearson correlation coefficients between aboveground biomass (AGB), belowground biomass (BGB), soil moisture at 0–5 cm depth (SM), soil temperature at 10 cm depth (T_S), and diurnal soil respiration rate (R_S) during the peak growing season of alpine grasslands in the Tibetan Plateau in 2006.[a]

	AGB	BGB	SM	T_S	R_S
AGB	1	0.78****	0.47**	−.36*	0.77****
BGB		1	0.64****	−0.44**	0.89****
SM			1	−0.69****	0.69****
T_S				1	−0.52***
R_S					1

[a] $n = 42$.
* $p < 0.05$.
** $p < 0.01$.
*** $p < 0.001$.
**** $p < 0.0001$.

3. Results

3.1. Soil respiration and field-measured factors

Table 1 describes the relationships among R_S and the field-measured factors. At the peak growing season of alpine grasslands, BGB showed the highest correlation with R_S ($r = 0.89$). The following was AGB and SM, with correlation coefficients (r) of 0.77 and 0.69, respectively. By contrast, T_S displayed relatively weak correlation with R_S (Table 1). Detailed explanation regarding the correlations between soil respiration and field-measured factors (i.e. AGB, BGB, SM, and T_S) can be found in Geng et al. (2012).

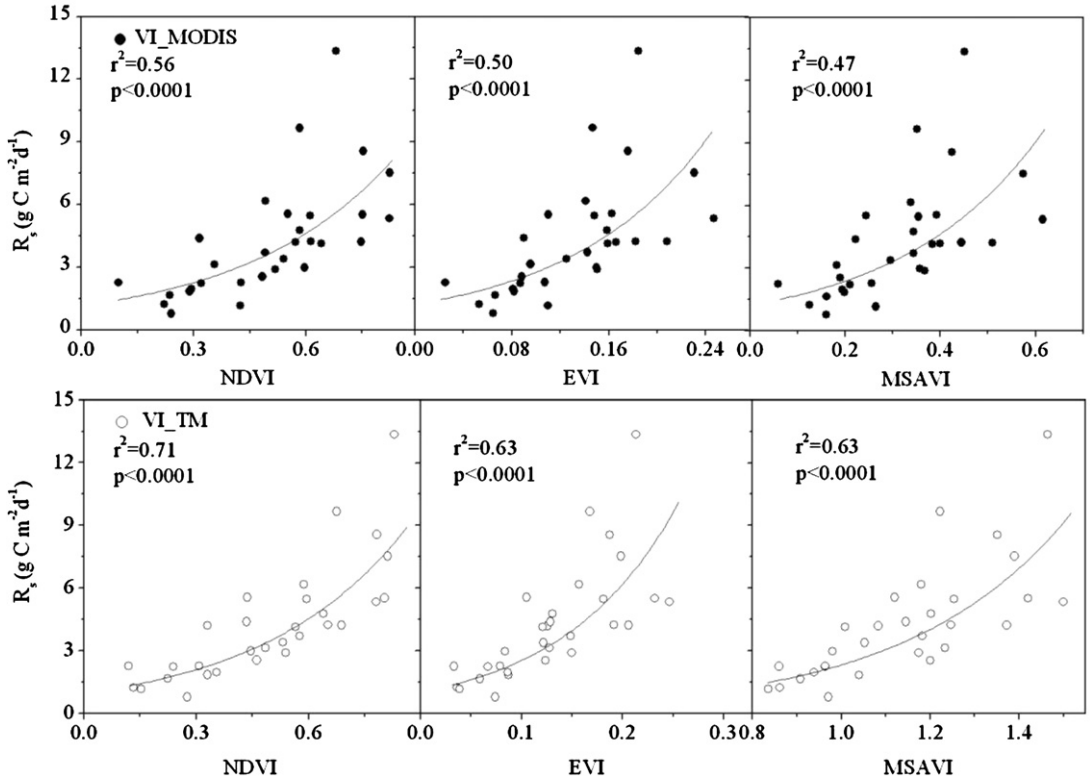

Fig. 3. Exponential relationships between diurnal soil respiration (R_S) and spectral vegetation indices (VIs) during the peak growing season of alpine grasslands in the Tibetan Plateau in 2006 ($n = 30$). VI_MODIS is the vegetation index (VI) calculated from the MODIS images, and VI_TM is the VI calculated from the Landsat TM images. The VIs are normalized difference vegetation index (NDVI), enhanced vegetation index (EVI), and modified soil adjusted vegetation index (MSAVI).

Author's personal copy

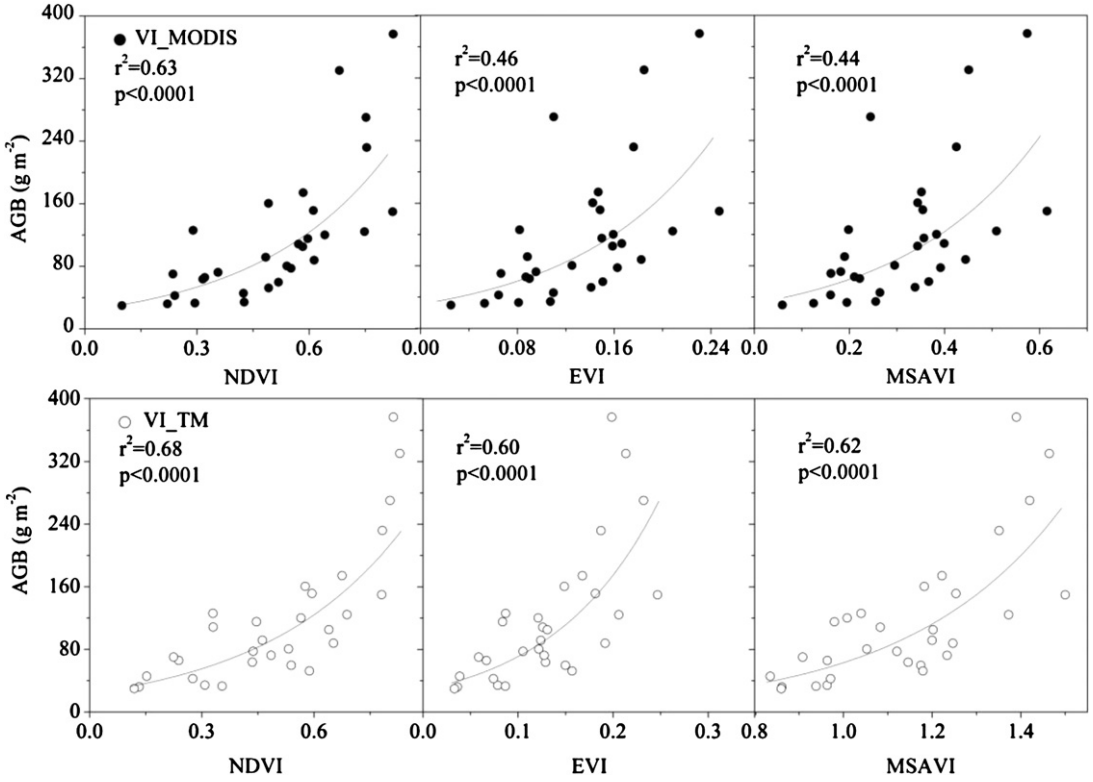

Fig. 4. Exponential relationships between aboveground biomass (AGB) and spectral vegetation indices (VIs) during the peak growing season of alpine grasslands in the Tibetan Plateau in 2006 ($n = 30$). See Fig. 3 caption for explanations of the VI_MODIS, VI_TM and VIs.

3.2. Relationships between soil respiration of alpine grasslands and spectral vegetation indices

The VIs (NDVI, EVI, and MSAVI) from the MODIS (VIs_MODIS) and Landsat TM (VIs_TM) consistently showed statistically significant relationships with R_S at the peak growing season of alpine grasslands in the Tibetan Plateau (Fig. 3). Moreover, exponential function was found to be the optimal function for describing the relationships among VIs and R_S. Based on either the MODIS or the TM images, the NDVI consistently showed higher explanatory power for R_S spatial variations than the EVI and the MSAVI. However, compared with the exponential model using NDVI_MODIS, the r^2 of the exponential model using NDVI_TM greatly improved from 0.56 to 0.71.

Similar to the correlation between the VIs and the R_S, the optimal fit functions for the relationships among the VIs and either AGB or BGB were also exponential functions (Figs. 4 and 5). Among the three VIs, the NDVI from either the MODIS or the TM is still the best estimator for the AGB or the BGB of alpine grasslands in the Tibetan Plateau. The NDVI_TM showed better correlation with the biomass of the alpine grasslands than the NDVI_MODIS. In addition, the coefficients of determination from the VI_MODIS or the VI_TM versus the BGB were consistently higher than those coefficients from their corresponding VI versus AGB (Figs. 4 and 5).

3.3. Mapping spatial patterns of soil respiration

As NDVI_TM was more powerful than the NDVI_MODIS for estimating R_S of the alpine grasslands, this index was subsequently used to estimate the spatial pattern of R_S at the peak growing season of alpine grasslands in the Tibetan Plateau. To achieve the scaling up from field plot-level measurements to the total plateau region, the NDVI_MODIS was first calibrated by using the NDVI_TM. The results showed that there was a good correlation between NDVI_MODIS and NDVI_TM ($r^2 = 0.83$) (Fig. 6). In accordance with the regression relationship between NDVI_MODIS and NDVI_TM (Fig. 6), we converted the NDVI_MODIS value into its corresponding NDVI_TM value. The final R_S prediction model for alpine grasslands was following:

$$R_S = 0.9805 \times e^{2.5763 \times (0.9655 \times \mathrm{NDVI\_MODIS} + 0.0166)}$$
$$r^2 = 0.71, \quad p < 0.0001 \tag{4}$$

where R_S was the diurnal soil respiration ($\mathrm{gC\,m^{-2}\,d^{-1}}$), NDVI_MODIS was the NDVI calculated from the MODIS images.

Then, based on the R_S prediction model (Eq. (4)), land use data, and MODIS 8-day composite reflectance product in the Tibetan Plateau, we derived the spatial patterns of R_S at the peak growing season of alpine grasslands (Fig. 7). The R_S of alpine grasslands was generally much higher in the southeastern part of the Tibetan Plateau and gradually decreased toward the northwestern part.

Fig. 8 shows the result of the accuracy assessment of the R_S prediction model. Field measured R_S was comparable to the calibrated NDVI_MODIS-estimated R_S. Based on the independent test dataset, calibrated NDVI_MODIS-estimated R_S accounted for 78% of spatial variation in ground measured R_S, and the RMSE is 1.45 $\mathrm{gC\,m^{-2}\,d^{-1}}$. The result of the accuracy assessment suggests that the prediction model, which used calibrated NDVI_MODIS as the dependent variable, is effective for the estimation of R_S.

4. Discussion

4.1. The relationships between alpine grassland biomass and spectral vegetation indices

Significant relationships were found among the VIs (NDVI, EVI, and MSAVI) and biomass (AGB and BGB) of the alpine grasslands in the Tibetan Plateau. This outcome is consistent with the results

Author's personal copy

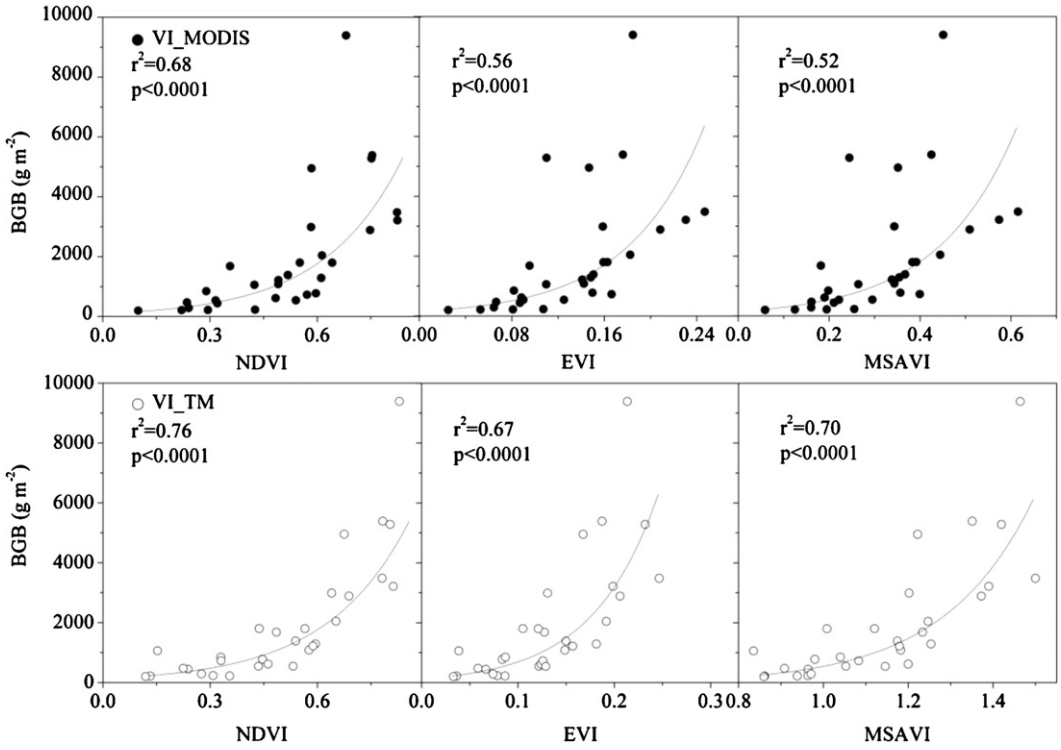

Fig. 5. Exponential relationships between belowground biomass (BGB) and spectral vegetation indices (VIs) during the peak growing season of alpine grasslands in the Tibetan Plateau in 2006 ($n = 30$). See Fig. 3 caption for explanations of the VI_MODIS, VI_TM and VIs.

obtained in the previous studies conducted on the same area (Chen et al., 2009; Yang et al., 2009). In comparison with the correlations between alpine grassland BGB and VIs, the correlations between AGB and VIs were consistently weaker (Figs. 4 and 5). This can be most likely attributed to the presence of senescent or dry vegetation. Non-photosynthetically active vegetation increases visible reflectance which limits the use of indices that dependent on the ratio between visible and near-infrared reflectance patterns (Todd et al., 1998; Brinkmann et al., 2011). Furthermore, remote sensing is usually used to estimate green vegetation cover and the VIs are indicative of green vegetation (Guo et al., 2011). When leaves senesce, the VIs may no longer aptly predict AGB (Huete et al., 1985; Marsett et al., 2006; Butterfield and Malmstrom, 2009). In this study, BGB is mainly vivid root biomass, which is closely related with the green part of aboveground vegetation. Therefore, these VIs were better correlated with BGB than with AGB.

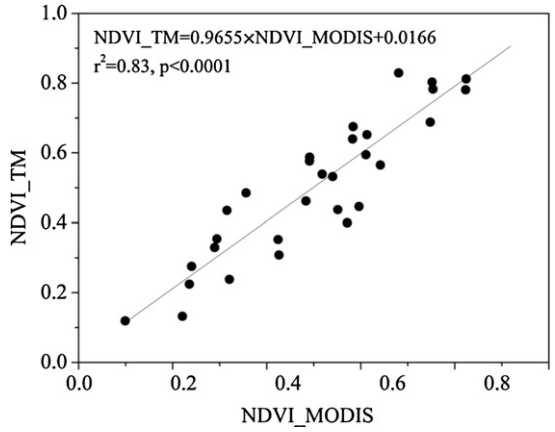

Fig. 6. Relationship between NDVI_MODIS (NDVI calculated from the MODIS images) and NDVI_TM (NDVI calculated from the Landsat TM images) during the peak growing season of alpine grasslands in the Tibetan Plateau in 2006 ($n = 30$).

The relationships among the VIs_MODIS and the biomass of alpine grassland (i.e. AGB and BGB) were consistently poorer than the relationships between the VIs_TM and AGB or BGB (Figs. 4 and 5). This may be due to the fact that coarse spatial resolution information (MODIS images) limited its usefulness for detailed studies in landscapes with heterogeneity at finer scales (Fisher and Mustard, 2007). A pixel in the 500 m resolution of MODIS images may cover multiple types of plant communities. These plant communities may have different species richness, soil texture, and topography conditions, which complicated the relationship between the biomass of alpine grasslands from small plot measurements and the spectral information of satellite (Butterfield and Malmstrom, 2009).

Furthermore, accurate image-based monitoring of plant ABG is limited by the effects of bare soil and vegetation clumping, which resulted in non-linear relationships between the measured signals and the biophysical properties of the vegetation (Huete et al., 1992; Paruelo and Lauenroth, 1995; Chen et al., 2009). Our study also demonstrated that the highest r^2 were achieved with nonlinear exponential models, but not linear model. This finding supported the findings of Hansen (1991), which showed a strong exponential relationship between NDVI and the biomass of Arctic and sub-Arctic vegetation types.

Moreover, our analysis revealed that the performance of biomass prediction of EVI and MSAVI, which were developed specifically to help accounting for the effects of background soil reflectance when vegetation is not fully covered (Qi et al., 1994; Huete et al., 2002), were not higher compared with the performance of NDVI. This might be explained by the estimated soil line parameters for MSAVI and added blue band for EVI, which were not substantially different from that assumed by the NDVI in the present study area. The same result was also found by Brinkmann et al. (2011) in semiarid rangelands. Therefore, NDVI seemed to

Author's personal copy

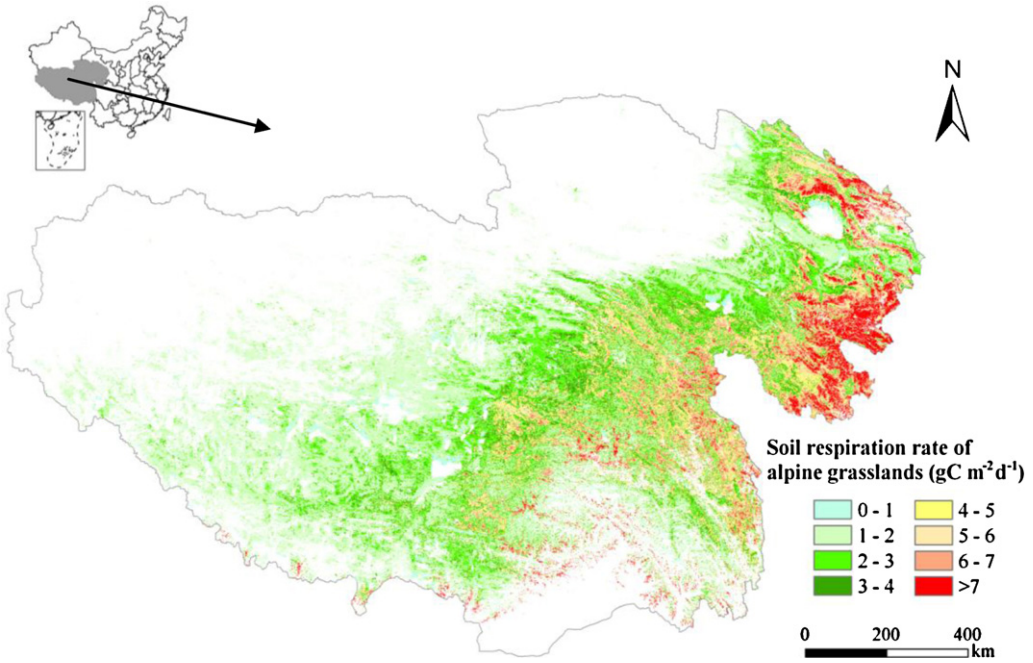

Fig. 7. Spatial patterns of soil respiration during the peak growing season of alpine grasslands in the Tibetan Plateau in 2006.

be the best predictor for AGB and BGB of alpine grasslands in the Tibetan Plateau, which confirms the reports of recent studies (Wylie et al., 2002; Zhao et al., 2007; Flynn et al., 2008; Brinkmann et al., 2011; Guo et al., 2011).

4.1.1. Spatial pattern of soil respiration in alpine grasslands

BGB can explain about 80% of the spatial variation in R_S (Table 1 and Geng et al., 2012), indicating that BGB is a major factor in influencing the spatial variation of R_S of alpine grasslands in the Tibetan Plateau. The reason may be that alpine grasslands have a high root biomass density (Yang et al., 2009). Thus, autotrophic respiration contributes a large proportion of the total respiratory CO_2 efflux, which has been discussed in detail by Geng et al. (2012).

In the Tibetan Plateau, R_S at the peak growing season of alpine grasslands showed varying values and spatial patterns. At the southeast, the distribution of alpine grasslands was concentrated and R_S was relatively high, but at the northwest, the distribution of alpine grasslands was sparse and the value of R_S was low. The reason may be attributed to the quantity and quality variation in the biomass of the alpine grasslands in the Tibetan Plateau area. For the alpine grasslands in the Tibetan Plateau, AGB and BGB were closely related (Yang et al., 2009). Furthermore, NDVI was found to be an effective tool to study the changes in the vegetation cover in the Tibetan Plateau (Ding et al., 2007; Zhou et al., 2007; Zhong et al., 2010), supporting our results that NDVI is the best predictor for AGB and BGB of the alpine grasslands. In addition, the spatial pattern of AGB of the alpine grasslands was in accordance with the climatic conditions in the Tibetan Plateau, which made the southeastern part more suitable for vegetation growth than the northwestern part (Niu et al., 2004; Zhou et al., 2007; Zhong et al., 2010). Yang et al. (2009) also found that the AGB of the alpine grasslands exhibit a gradually decreasing trend from the southeast to northwest due to the growing season precipitation in the Tibetan Plateau. The same phenomenon was also observed in the temperate grasslands in arid and semi-arid regions in China (Fu et al., 2006; Jin et al., 2009). These findings provide a suitable explanation for the spatial pattern of R_S at the mid-growing season of alpine grasslands in the Tibetan Plateau.

The accuracy of this method, with a r^2 of 0.78 and a RMSE of 1.45 gC m^{-2} d^{-1}, is slightly lower than the accuracy estimations of the R_S in a tropical grassland (Caquet et al., 2012) and in an oak forest (Joo et al., 2012). The accuracy is also comparable to the estimation of R_S in a paddy ecosystem (Ren et al., 2007). However, our method is largely superior to methods which are based only on field measurements. For instance, our method can answer large-scale questions about the regional variation of R_S at the peak growing season of alpine grasslands at very low cost (all the satellite data used here are available for free) compared to observations of field plots at the local level. In addition to its immediate applications for regional estimation of R_S, our large-scale estimation of R_S method can be a useful scientific tool for research work that aim to understand the R_S response of alpine grasslands to global warming, especially in the climate-sensitive Tibetan Plateau (Zhou et al., 2007; Kang et al., 2010; Zhao et al., 2011; Zhong et al., 2011).

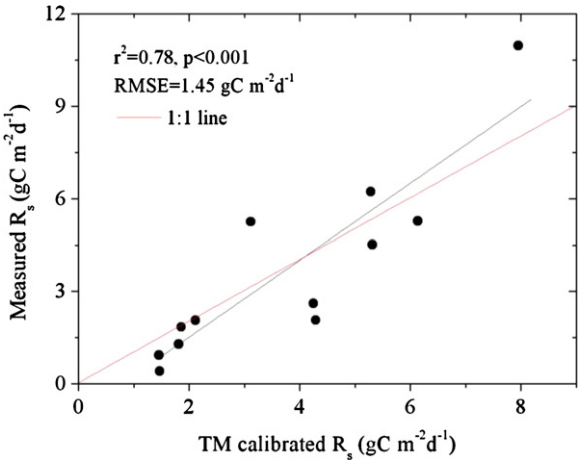

Fig. 8. TM-calibrated NDVI_MODIS-estimated soil respiration (R_S) and corresponding ground-based measurements with r^2 and RMSE (gC m^{-2} d^{-1}) during the peak growing season of alpine grasslands in the Tibetan Plateau in 2006 (n = 12).

Author's personal copy

4.1.2. Soil respiration field measurement

Problems may be inherent in using the soil flux chamber, as it allowed us to measure only the R_s taking place through the soil surface within a PVC soil collar (10 cm inside diameter and 5 cm in height). We were limited in our ability to estimate the soil CO_2 flux of the entire stand, although five to seven PVC soil collars were placed along a straight line at one-meter intervals to derive the plot-level R_s value. This problem was compounded when the R_s from soil flux chamber were compared to the satellite images. For example, in the MODIS 8-day composite reflectance image, each pixel represents an area of 500 m × 500 m and includes different plant communities and soil conditions. The relative contributions of these sources of R_s are important, but they cannot be measured through this method. We used the 30 m resolution of Landsat TM image to calibrate the coarse resolution MODIS images, which reduced the effect of mixed pixels to a certain extent. This research certainly needs to be continued in other ecosystems. Until a valid method to measure the R_s over a large spatial scale is established, the application of a small, portable, and more affordable soil flux chamber is still a good method for studying the spatial patterns of R_s.

4.1.3. Uncertainties

In this study, we focused our analysis on the peak growing season of alpine grasslands. Therefore, the results may be not suitable for non-growing season or in regions where R_s is controlled mainly by other factors, such as temperature, moisture, soil organic carbon content, and other factors. In addition, the MODIS images used in this current study formed a good source of data because we were able to achieve full coverage of the entire study area with high-quality data. However, the spatial resolution of 500 m was relatively coarse, although we used the high spatial resolution Landsat TM images to calibrate the MODIS images. This creates another source of uncertainty.

5. Conclusion

A remote sensing-based method was developed to estimate the spatial pattern of R_s in the alpine grasslands in the Tibetan Plateau. The method used was based on the result of a recent study (Geng et al., 2012) that BGB is the most important driving factor for large-scale variations in R_s at the peak growing season of alpine grasslands in the Tibetan Plateau. By selecting VIs that have potential for estimating plant biomass, we examined the capacity of VIs from Landsat TM and MODIS images to predict the spatial variation in R_s in the alpine grasslands in the Tibetan Plateau.

Based on the remote-sensing data from either MODIS or Landsat TM, the exponential function was found to be the optimal fit function for describing the relationships among the VIs and the R_s. The VIs_TM consistently showed better relationships with R_s than VIs_MODIS. Moreover, NDVI consistently showed higher accuracy in estimating the spatial variation of R_s than the EVI and the MSAVI. Thus, the exponential function of NDVI_TM versus R_s was used as the predicting model to estimate the spatial patterns of R_s of the alpine grasslands. However, as the Landsat TM images are difficult to achieve full coverage of the whole study area, we calibrated the NDVI_MODIS using the NDVI_TM by converting the NDVI_MODIS into its corresponding NDVI_TM. Then, based on the 500 m-resolution MODIS 8-day surface reflectance product and land cover data in the Tibetan Plateau, we estimated the spatial variations of the R_s during the peak growing season of alpine grasslands using the TM-calibrated R_s prediction model. The calibrated NDVI_MODIS-estimated R_s agreed well with ground measurements based on the independent test samples.

As the alpine grasslands have a high root biomass density at the peak growing season, the autotrophic respiration contributes a large proportion of the total R_s, and BGB explains the great spatial variation of the R_s. Thus, the VIs correlated with the BGB can be used to estimate R_s. The results should have implications for other vegetation types which have similar physiological conditions as the alpine grasslands. Using the NDVI, the R_s of alpine grasslands can be predicted from the remote sensing data and can be upscaled using remotely sensed data.

Understanding and predicting the spatial variability of R_s is a key issue in parameterizing grassland ecosystems in global vegetation models. Therefore, cross-ecosystem comparisons of R_s and optical properties are essential to explore and scale the soil CO_2 flux of grasslands. Further analyses are also required to investigate the relationships between R_s and VIs at an early or later growing season from different satellite platforms.

Acknowledgements

We sincerely thank the anonymous reviewers for their important and constructive revision advices on the manuscript. This work was supported by the Major State Basic Research Development Program of China (2010CB950603), the Major State Basic Research Development Program of China (2010CB950602), the Major State Basic Research Development Program of China (2013CB733405), Public service sectors (meteorology) Special Fund Research (GYHY201006042), and National Natural Science Foundation of China (41201345).

References

Bader, N.E., Cheng, W.X., 2007. Rhizosphere priming effect of *Populus fremontii* obscures the temperature sensitivity of soil organic carbon respiration. Soil Biol. Biochem. 39, 600–606.

Balogh, J., Pinter, K., Foti, S., Cserhalmi, D., Papp, M., Nagy, Z., 2011. Dependence of soil respiration on soil moisture, clay content, soil organic matter, and CO_2 uptake in dry grasslands. Soil Biol. Biochem. 43, 1006–1013.

Brinkmann, K., Dickhoefer, U., Schlecht, E., Buerkert, A., 2011. Quantification of aboveground rangeland productivity and anthropogenic degradation on the Arabian Peninsula using Landsat imagery and field inventory data. Remote Sens. Environ. 115, 465–474.

Butterfield, H.S., Malmstrom, C.M., 2009. The effects of phenology on indirect measures of aboveground biomass in annual grasses. Int. J. Remote Sens. 30, 3133–3146.

Caquet, B., De Grandcourt, A., M'bou, A.T., Epron, D., Kinana, A., Saint Andre, L., Nouvellon, Y., 2012. Soil carbon balance in a tropical grassland: Estimation of soil respiration and its partitioning using a semi-empirical model. Agric. Forest Meterol. 158, 71–79.

Chen, J., Gu, S., Shen, M.G., Tang, Y.H., Matsushita, B., 2009. Estimating aboveground biomass of grassland having a high canopy cover: an exploratory analysis of in situ hyperspectral data. Int. J. Remote Sens. 30, 6497–6517.

Chen, X.W., Post, W.M., Norby, R.J., Classen, A.T., 2011. Modeling soil respiration and variations in source components using a multi-factor global climate change experiment. Climatic Change 107, 459–480.

Cleland, E.E., Chiariello, N.R., Loarie, S.R., Mooney, H.A., Field, C.B., 2006. Diverse responses of phenology to global changes in a grassland ecosystem. Proc. Natl. Acad. Sci. U. S. A. 103, 13740–13744.

Cox, P.M., Betts, R.A., Jones, C.D., et al., 2000. Acceleration of global warming due to carbon-cycle feedbacks in a coupled climate model. Nature 408, 184–187.

Craine, J.M., Wedin, D.A., Chapin, F.S., 1999. Predominance of ecophysiological controls on soil CO_2 flux in a Minnesota grassland. Plant Soil 207, 77–86.

de Graaff, M.A., Classen, A.T., Castro, H.F., Schadt, C.W., 2010. Labile soil carbon inputs mediate the soil microbial community composition and plant residue decomposition rates. New Phytol. 188, 1055–1064.

Ding, M.J., Zhang, Y.L., Liu, L.S., Zhang, W., Wang, Z.F., Bai, W.Q., 2007. The relationship between NDVI and precipitation on the Tibetan Plateau. Journal of Geographical Sciences 17, 259–268.

Fang, C., Moncrieff, J.B., Gholz, H.L., Clark, K.L., 1998. Soil CO_2 efflux and its spatial variation in a Florida slash pine plantation. Plant Soil 205, 135–146.

Fisher, J.I., Mustard, J.F., 2007. Cross-scalar satellite phenology from ground, Landsat, and MODIS data. Remote Sens. Environ. 109, 261–273.

Flynn, E.S., Dougherty, C.T., Wendroth, O., 2008. Assessment of pasture biomass with the normalized difference vegetation index from active ground-based sensors. Agron. J. 100, 114–121.

Author's personal copy

Fu, Y.L., Yu, G.R., Wang, Y.F., Li, Z.Q., Hao, Y.B., 2006. Effect of water stress on ecosystem photosynthesis and respiration of a Leymus chinensis steppe in Inner Mongolia. Sci. China Ser.—Earth Sci. 49, 196–206.
Geng, Y., Wang, Y., Yang, K., Wang, S., Zeng, H., Baumann, F., Kuehn, P., Scholten, T., He, J.S., 2012. Soil respiration in Tibetan alpine grasslands: belowground biomass and soil moisture, but not soil temperature, best explain the large-scale patterns. PLoS One 7, e34968, http://dx.doi.org/10.1371/journal.pone.0034968.
Guo, X.L., Black, S.C., He, Y.H., 2011. Estimation of leaf CO_2 exchange rates using a SPOT image. Int. J. Remote Sens. 32, 353–366.
Han, G.X., Zhou, G.S., Xu, Z.Z., Yang, Y., Liu, J.L., Shi, K.Q., 2007. Biotic and abiotic factors controlling the spatial and temporal variation of soil respiration in an agricultural ecosystem. Soil Biol. Biochem. 39, 418–425.
Hansen, B.U., 1991. Monitoring natural vegetation in southern Greenland using NOAA AVHRR and field measurements. Arctic 44, 94–101.
Högberg, P., Nordgren, A., Buchmann, N., Taylor, A.F.S., Ekblad, A., Högberg, M.N., et al., 2001. Large-scale forest girdling shows that current photosynthesis drives soil respiration. Nature 411, 789–792.
Huang, N., Niu, Z., Wu, C.Y., Tappert, M.C., 2010. Modeling net primary production of a fast-growing forest using a light use efficiency model. Ecol. Model. 221, 2938–2948.
Huete, A., Didan, K., Miura, T., Rodriguez, E.P., Gao, X., Ferreira, L.G., 2002. Overview of the radiometric and biophysical performance of the MODIS vegetation indices. Remote Sens. Environ. 83, 195–213.
Huete, A.R., 1988. A soil-adjusted vegetation index (SAVI). Remote Sens. Environ. 83, 195–213.
Huete, A.R., Hua, G., Qi, J., Chehbouni, A., van Leeuwen, W.J.D.G., 1992. Normalization of multidirectional red and NIR reflectances with the SAVI. Remote Sens. Environ. 41, 143–154.
Huete, A.R., Jackson, R.D., Post, D.F., 1985. Spectral response of a plant canopy with different soil backgrounds. Remote Sens. Environ. 17, 37–53.
Jin, Z., Qi, Y.C., Dong, Y.S., Domroes, M., 2009. Seasonal patterns of soil respiration in three types of communities along grass–desert shrub transition in Inner Mongolia, China. Adv. Atmos. Sci. 26, 503–512.
Joo, S.J., Park, S.U., Park, M.S., Lee, C.S., 2012. Estimation of soil respiration using automated chamber systems in an oak (*Quercus mongolica*) forest at the Nam-San site in Seoul, Korea. Sci. Total Environ. 416, 400–409.
Kang, S.C., Xu, Y.W., You, Q.L., Flugel, W.A., Pepin, N., Yao, T.D., 2010. Review of climate and cryospheric change in the Tibetan Plateau. Environ. Res. Lett. 5, 015101, http://dx.doi.org/10.1088/1748-9326/5/1/015101.
Kuzyakov, Y., Larionova, A.A., 2005. Root and rhizomicrobial respiration: a review of approaches to estimate respiration by autotrophic and heterotrophic organisms in soil. J. Plant Nutr. Soil Sci. 168, 503–520.
Li, W.H., Zhou, X.M., 1998. Ecosystems of Qinghai-Xizang (Tibetan) Plateau and Approach for their Sustainable Management. Guangdong Science and Technology Press, Guangzhou.
Marsett, R.C., Qi, J.G., Heilman, P., Biedenbender, S.H., Watson, M.C., Amer, S., Weltz, M., Goodrich, D., Marsett, R., 2006. Remote sensing for grassland management in the arid Southwest. Rangeland Ecol. Manage. 59, 530–540.
Moyano, F.E., Kutsch, W., Schulze, E-D., 2007. Response of mycorrhizal, rhizosphere and soil basal respiration to temperature and photosynthesis in a barley field. Soil Biol. Biochem. 39, 843–853.
Niu, T., Chen, L.X., Zhou, Z.J., 2004. The characteristics of climate change over the Tibetan Plateau in the last 40 years and the detection of climatic jumps. Adv. Atmos. Sci. 21, 193–203.
Ouyang, W., Hao, F.H., Skidmore, A.K., Groen, T.A., Toxopeus, A.G., Wang, T.J., 2012. Integration of multi-sensor data to assess grassland dynamics in a Yellow River sub-watershed. Ecol. Indic. 18, 163–170.
Paruelo, J.M., Lauenroth, W.K., 1995. Regional patterns of normalized difference vegetation index in North American shrublands and grasslands. Ecology 76, 1888–1898.
Pendall, E., Leavitt, S.W., Brooks, T., Kimball, B.A., Pinter, P.J., Wall, G.W., et al., 2001. Elevated CO_2 stimulates soil respiration in a FACE wheat field. Basic Appl. Ecol. 2, 193–201.
Qi, J., Chehbouni, A., Huete, A.R., Kerr, Y.H., Sorooshian, S., 1994. A modified soil adjusted vegetation index (MSAVI). Remote Sens. Environ. 48, 119–126.
Raich, J.W., Schlesinger, W.H., 1992. The global carbon dioxide flux in soil respiration and its relationship to vegetation and climate. Tellus Series B—Chem. Phys. Meteorol. 44, 81–99.
Reeves, M.C., Zhao, M.S., Running, S.W., 2006. Applying improved estimates of MODIS productivity to characterize grassland vegetation dynamics. Rangeland Ecol. Manage. 59, 1–10.
Ren, X.E., Wang, Q.X., Tong, C.L., Wu, J.S., Wang, K.L., Zhu, Y.L., Lin, Z.J., Masataka, W., Tang, G.Y., 2007. Estimation of soil respiration in a paddy ecosystem in the subtropical region of China. Chin. Sci. Bull. 52, 2722–2730.
Rouse, J.W., Haas, R.H., Schell, J.A., Deering, D.W., Harlan, J.C., 1974. Monitoring the vernal advancements and retrogradation of natural vegetation. In: NASA/GSFC, Final Report, Greenbelt, MD, USA, pp. 1–137.
Schlesinger, W.H., Andrews, J.A., 2000. Soil respiration and the global carbon cycle. Biogeochemistry 48, 7–20.
Scurlock, J.M.O., Hall, D.O., 1998. The global carbon sink: a grassland perspective. Global Change Biol. 4, 229–233.
Tang, J.W., Baldocchi, D.D., Xu, L., 2005. Tree photosynthesis modulates soil respiration on a diurnal time scale. Global Change Biol. 11, 1298–1304.
Todd, S.W., Hoffer, R.M., Milchunas, D.G., 1998. Biomass estimation on grazed and ungrazed rangelands using spectral indices. Int. J. Remote Sens. 19, 427–438.
Trumbore, S., 2006. Carbon respired by terrestrial ecosystems-recent progress and challenges. Global Change Biol. 12, 141–153.
Vogelman, J.E., Howard, S.M., Yang, L.M., Larson, C.R., Wylie, B.K., Van Driel, N., 2001. Completion of the 1990 National Land Cover Data set for the conterminous United States for Landsat Thematic Mapper data and ancillary data sources. Photogramm. Eng. Remote Sens. 67, 650–662.
Wylie, B.K., Meyer, D.J., Tieszen, L.L., Mannel, S., 2002. Satellite mapping of surface biophysical parameters at the biome scale over the North American grasslands—a case study. Remote Sens. Environ. 79, 266–278.
Yang, M.X., Yao, T.D., Gou, X.H., Wang, H.J., Ha, L.S., 2007. Comparison analysis of the summer monsoon precipitation between northern and southern slopes of Tanggula Mountains, Qinghai-Xizang (Tibetan) Plateau: a case study in summer 1998. Hydrol. Process. 21, 1841–1847.
Yang, Y.H., Fang, J.Y., Pan, Y.D., Ji, C.J., 2009. Aboveground biomass in Tibetan grasslands. J. Arid Environ. 73, 91–95.
Zhao, D.H., Huang, L.M., Li, J.L., Qi, J.G., 2007. A comparative analysis of broadband and narrowband derived vegetation indices in predicting LAI and CCD of a cotton canopy. Int. Soc. Photogramm. Remote Sens. 62, 25–33.
Zhao, D.S., Wu, S.H., Yin, Y.H., Yin, Z.Y., 2011. Vegetation distribution on Tibetan Plateau under climate change scenario. Regional Environ. Change 11, 905–915.
Zhong, L., Ma, Y.M., Salama, M.S., Su, Z.B., 2010. Assessment of vegetation dynamics and their response to variations in precipitation and temperature in the Tibetan Plateau. Climate Change 103, 519–535.
Zhong, L., Su, Z.B., Ma, Y.M., Salama, M.S., Sobrino, J.A., 2011. Accelerated changes of environmental conditions on the Tibetan Plateau caused by climate change. J. Climate 24, 6540–6550.
Zhou, D.W., Fan, G.Z., Huang, R.H., Fang, Z.F., Liu, Y.Q., Li, H.Q., 2007. Interannual variability of the normalized difference vegetation index on the Tibetan Plateau and its relationship with climate change. Adv. Atmos. Sci. 24, 474–484.